1,1'-Bis(diphenylphosphino)ferrocene bridging two mono(cyclopentadienyl) cobalt moieties: Synthesis, structure, electrochemistry and DFT studies

9 AUTHORS, INCLUDING:

Vitor Rosa
New University of Lisbon
32 PUBLICATIONS **304** CITATIONS

SEE PROFILE

Sara Realista
University of Lisbon
5 PUBLICATIONS **5** CITATIONS

SEE PROFILE

Ana Cristina Mourato
University of Lisbon
12 PUBLICATIONS **175** CITATIONS

SEE PROFILE

1,1′-Bis(diphenylphosphino)ferrocene bridging two mono(cyclopentadienyl) cobalt moieties: Synthesis, structure, electrochemistry and DFT studies

Vitor Rosa [a], Sara Realista [b], Ana Mourato [b], Luisa Maria Abrantes [b], João Henriques [b], Maria José Calhorda [b,**], Teresa Avilés [a,*], Michael G.B. Drew [c], Vitor Félix [d]

[a] REQUIMTE/CQFB Departamento de Química, Faculdade de Ciências e Tecnologia, Universidade Nova de Lisboa, 2825-516 Caparica, Portugal
[b] Departamento de Química e Bioquímica, CQB, Faculdade de Ciências, Universidade de Lisboa, Campo Grande, 1749-016 Lisboa, Portugal
[c] Department of Chemistry, University of Reading, Whiteknights, Reading RG6 6AD, UK
[d] Departamento de Química, CICECO and Secção Autónoma de Ciências da Saúde, Universidade de Aveiro, 3810-193 Aveiro, Portugal

ARTICLE INFO

ABSTRACT

Reaction of $[Co(\eta^5-C_5H_5)(CO)_2]$, **1**, with 1,1′-bis(diphenylphosphino)ferrocene (dppf) yields the new trinuclear complex $[Co(\eta^5-C_5H_5)(CO)]_2(\mu\text{-dppf})$, **2**, which was structurally characterised by single crystal X-ray diffraction and showed two $Co(\eta^5-C_5H_5)(CO)$ moieties covalently linked by a dppf bridge. Electrochemical studies in dichloromethane revealed that both Co(I) and Fe(II) in the precursors were oxidized to Co(II)/Co(III) and Fe(III), respectively. On the other hand, in **2** the two first oxidation waves were assigned to Co, the Fe(II) centre requiring a higher potential than in free dppf. DFT calculations showed that the HOMOs of **2** were localised in the Co fragments, owing to the destabilisation of the $Co(\eta^5-C_5H_5)(CO)$ orbitals after binding dppf.

© 2012 Elsevier B.V. All rights reserved.

1. Introduction

Cobalt complexes of type CpCoL$_2$ (L = CO, PR$_3$, alkenes) have been extensively used as catalysts, one of the most important applications being the cocyclizations of alkynes [1], a reaction known for more than three decades but still attracting a lot of attention; several studies regarding the mechanism of this reaction have being recently published [2]. We have being interested in the chemistry of the monocyclopentadienyl cobalt moiety for a number of years [3] and also in the use of the ligand 1,1′-bis(diphenylphosphino)ferrocene (dppf) [4]. The use of dppf as a ligand in coordination chemistry is well developed, as it coordinates to a variety of transition metals in several ways, such as monodentate, chelate and bridging. Also, dppf is a metallo-ligand giving rise to binuclear complexes that exhibit a reactivity different from that of their mononuclear analogues, as they can undergo sequential electron-transfer steps leading to unusual catalytic activity [5]. Sometime ago, we studied the reaction of dppf with $[Co(\eta^5-C_5H_5)(CO)I_2]$ [6] and observed that dppf acted as chelate, forming $[Co(\eta^5-C_5H_5)(dppf)I]I$, or as a bridging ligand between two Co centres. Interestingly, the study of the magnetic properties of the resulting chain compound revealed a behaviour typical of Co(II) in a tetrahedral environment, the highest occupied orbitals being localised in cobalt rather than in iron. In order to expand the synthesis of new ferrocene based heterobimetallic compounds, the reaction of dppf with $[Co(\eta^5-C_5H_5)(CO)_2]$ (**1**) was performed, leading to the polynuclear complex $[Co(\eta^5-C_5H_5)(CO)]_2(\mu\text{-dppf})$ (**2**). The structure of **2** was determined by single crystal X-ray diffraction studies, showing two $Co(\eta^5-C_5H_5)(CO)$ moieties covalently linked by a bridging ligand. Electrochemical studies were performed in order to study the redox behaviour of this trinuclear complex and DFT calculations [7] were performed to rationalise the results.

2. Experimental

2.1. General procedures and materials

All reactions and manipulations of solutions were performed under an argon atmosphere using Schlenk techniques. Solvents were reagent grade and dried according to literature methods. Co$_2$(CO)$_8$ was purchased from Fluka and used as supplied. The ligand 1,1′-bis(diphenylphosphino)ferrocene (dppf) [8] and the

complex $Co(\eta^5\text{-}C_5H_5)(CO)_2$ [9] were prepared as previously reported. Infrared spectra were recorded as mulls on NaCl plates using an ATI Mattson Genesis FTIR spectrometer. Elemental analyses were performed at the Analytical services of the Laboratory of REQUIMTE of the Universidade Nova de Lisboa, Portugal. ^1H and ^{31}P NMR spectra were recorded on an NMR Bruker ARX 400. ^1H NMR spectra were recorded using TMS as internal reference; ^{31}P shifts were measured with respect to external 85% H_3PO_4.

2.2. Synthesis of $[Co(\eta^5\text{-}C_5H_5)(CO)]_2(\mu\text{-}dppf)$ **2**

A solution of dppf (1.17 g, 2.11 mmol) in toluene (40 mL) was added to a solution of $Co(\eta^5\text{-}C_5H_5)(CO)_2$ (0.76 g, 4.22 mmol) in toluene (10 mL), magnetically stirred at room temperature. Gas evolution was immediately observed (presumably CO), no appreciable colour change was observed, the solution maintaining an intense red colour, and was left under stirring 12 h at reflux. The solution was concentrated by vacuum removal of the solvent, and petroleum ether was added until the solution became turbid. After filtration the remaining solution was put in the refrigerator affording, after 2 days, red crystals that were washed with petroleum ether, and dried in vacuum to give pure **2**. (Yield 85%) (Found: C, 63.55; H, 4.78 Calc. for $C_{46}H_{38}CoFeP_2O_2$: C, 63.37; H, 4.43). NMR (C_6D_6): ^1H, δ 7.76–7.02 (m, 20 H, Ph), 4.60 (s, 10H, C_5H_5), 4.53 (s, 4H, C_5H_4), 4.46 (s, 4H, C_5H_4), ^{31}P, δ 61.63 (s). I.R. (nujol mull), $\nu_{CO} = 1913$ cm^{-1}.

2.3. Crystallography

Red crystals of $[Co(\eta^5\text{-}C_5H_5)(CO)]_2(\mu\text{-}dppf)_2)$ **(2)** suitable for single crystal X-ray determination were grown up from a toluene/petroleum ether solution. Crystal data: $C_{46}H_{38}Co_2FeO_2P_2$, $Mr = 858.41$; triclinic space group $P\bar{1}$, $Z = 2$, $a = 10.595(12)$, $b = 14.471(17)$, $c = 14.236(18)$ Å, $\alpha = 63.95(1)$, $\beta = 83.91(1)$ $\gamma = 79.80(1)°$, $V = 1928.9$ Å^3, $\rho(calc) = 1.478$ Mg m^{-3}, $\mu = 1.343$ mm^{-1}.

X-ray data were collected at room temperature on a MAR research plate system using graphite monochromatised Mo-Kα radiation ($\lambda = 0.71073$ Å) at Reading University. The crystal was positioned at 70 mm from the image plate. 95 frames were taken at $2°$ intervals using an appropriate counting time. Data analysis was performed with the XDS program [10]. Intensities were corrected for absorption effects using the DIFABS program modified for the image plate geometry [11].

The structure was solved by direct methods and by subsequent difference Fourier syntheses and refined by full matrix least squares on F^2 using the SHELX-97 system programs [11]. Anisotropic thermal parameters were used for the remaining non-hydrogen atoms. The hydrogen atoms bonded to carbon were included in refinement in calculated positions with isotropic parameters equivalent 1.2 times those of the atom to which were attached. The residual electronic density ranging from -0.813 to 0.955 eÅ^{-3} was within expected values. The final refinement of 464 parameters converged to final R and R_w indices $R_1 = 0.0860$ and $wR_2 = 0.2234$ for 2165 reflections with $I > 2\sigma(I)$, and $R_1 = 0.1843$, and $wR_2 = 0.2736$ for all 4576 hkl data. Molecular diagrams presented are drawn with graphical package software PLATON [12]; CCDC reference number: 614689.

2.4. Electrochemical studies

The electrochemical measurements were performed using a CHI Electrochemical Analyser-620A Model controlled by a computer and a one-compartment cell. A polycrystalline platinum working electrode was used in all conventional electrochemical experiments. A Pt foil and a saturated calomel electrode (SCE) were used as counter and reference electrode, respectively.

The solution volumes were ca. 5 mL with a concentration of ca. 10^{-3} M of complex **2**, and precursors (dppf and **1**) in 0.1 M of TBAPF$_6$ in dichloromethane, prepared in a N$_2$-filled Vacuum Atmospheres dry box. Dichloromethane (HPLC grade, Aldrich 99.93%) was previously dried in calcium hydride and distilled with phosphorus pentoxide under N$_2$ atmosphere. Tetrabutylammonium hexafluorophosphate, TBAPF$_6$ (Fluka, puriss. $\geq$ 99%), was previously recrystallised from ethanol.

2.5. Computational studies

DFT calculations [7] were performed using the Gaussian 03 software package [13], and the B3LYP functional [14–17], without symmetry constraints and a tight self-consistent field (SCF) convergence criteria. This functional uses Becke's three parameter hybrid functional [14], non-local correlation provided by the LYP expression [15], and the VWN functional III [16] for local correlation. VWN is used to provide the excess local correlation required, since LYP contains a local and non-local term equivalent to VWN. The optimised geometries were obtained with LANL2TZ basis set [18] augmented with an f-polarisation function for Co and Fe, and a standard 6-31G(d,p) [19–23], for the remaining elements. Frequency calculations were performed to confirm the nature of the stationary points. Whenever a frequency calculation yielded imaginary frequencies the optimisation procedure was repeated using the Gaussian keyword CalcFC. This specifies that the force constants are to be computed explicitly at the first step of the geometry optimization procedure, bypassing the default construction of an approximate Hessian.

Solvent effects were considered using the Polarizable Continuum Model (PCM) initially devised by Tomasi and coworkers [24–26] as implemented on Gaussian 03 [27,28]. The molecular cavity was constructed using the Bondi atomic radii [29]. According to the experimental procedures, the solvent used was dichloromethane.

The structures were modelled after the crystal structure of complex **2** described in this work. Three-dimensional representations of the orbitals were obtained with Molekel [30].

3. Results and discussion

3.1. Chemical and crystallographic studies

Reaction of $[Co(\eta^5\text{-}C_5H_5)(CO)_2]$ with 1,1′-bis(diphenylphosphino)ferrocene (dppf) in toluene yielded the new polynuclear compound $[Co(\eta^5\text{-}C_5H_5)(CO)]_2(\mu\text{-}dppf)$, **2**, (see Scheme 1). The structure of this complex was determined by single crystal X-ray diffraction studies, showing two $Co(\eta^5\text{-}C_5H_5)(CO)$ complex units linked by a dppf bridge. Some compounds where dppf bridges two $Fe(\eta^5\text{-}C_5H_5)$ [31] or $Rh(\eta^5\text{-}C_5H_5)$ moieties [32] have been described. In the compound $Mn(\eta^5\text{-}CH_3C_5H_4)(CO)_2(dppf)$ [33], however, the ligand dppf is monodentate.

The molecular diagram of $[Co(\eta^5\text{-}C_5H_5)(CO)]_2(\mu\text{-}dppf)$ showing two $Co(\eta^5\text{-}C_5H_5)(CO)$ complex units linked by a dppf bridge is presented in Fig. 1. The two Cp rings of the bridging ligand adopt an almost eclipsed arrangement leading to a *trans* disposition of the two phosphorus donor atoms with a P(1)–C(41)···C(53)-(P2) dihedral angle of $-131.6(8)°$. The two Co centres are 7.605(3) Å apart, while the Co···Fe distances are 4.928(3) and 4.746(3) Å, respectively. These intermolecular distances prevent through the space electronic communication between any pairs of metal centres.
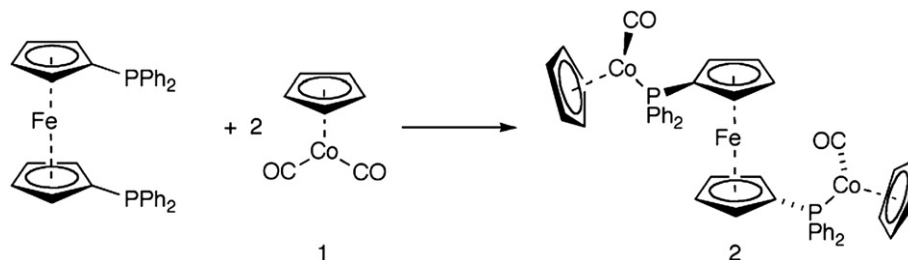
Scheme 1.

A search on the Cambridge Structural Database [34] shows a structure (refcode WIBBIS) [35] in which a dppf ligand is directly bridging two (μ^2-ethylidyne)-octacarbonyl-tri-cobalt cluster units in a comparable geometric arrangement. However, the intermolecular distance of 9.84 Å between the two cobalt centres bonded to the phosphorus donors is longer than that found for **2**. The Fe⋯Co distances for this complex are 4.921 Å. The selected bond distances and angles for **2** are listed in Table 1. The two carbonyl groups are bonded linearly to the cobalt centres with Co–C distances of 1.683(14) and 1.678(7) Å and Co–C≡O angles of 179.0(12) and 178.2(4)°, respectively. The coordination geometry around each cobalt centre considering the centroid of the η^5-Cp ring, the carbonyl group and the phosphorus donor atom is distorted triangular. All bond lengths and angles found in the crystal structure are within the expected values.

3.2. Electrochemical studies

Cyclic voltammetry was used to evaluate the redox process for the three complexes, $[Co(\eta^5-C_5H_5)(CO)_2]$ (**1**), dppf, and $[Co(\eta^5-C_5H_5)(CO)]_2(\mu\text{-dppf})$ (**2**). The voltammograms of the precursor dppf (Fig. 2A, a) show two irreversible oxidation peaks at 0.79 and 1.38 V, which correspond to the conversion of Fe(II) to Fe(III) and to decomposition of the compound, respectively. The electrochemical profile recorded for the Co containing precursor (Fig. 2A,b), within 0.1–0.9 V the potential range, displays two oxidation peaks which are related with the Co(I)/Co(II)/Co(III) conversions; for higher potential values the small peak observed at 1.05 V is due to the decomposition of the compound, as described by *Z*. Pang [36]. The redox pattern exhibited by the Co (I) derivative $[Co(\eta^5-C_5H_5)(CO)]_2(\mu\text{-dppf})$ (**2**), in dichloromethane solution is depicted in Fig. 2B. The two oxidation processes that occur at 0.38 and 0.95 V are assigned to the oxidations of Co(I) to Co(II) and Co(II) to Co(III), respectively, whereas the reversible oxidation at the further

positive domain (ca 1.23 V) is due to the oxidation of dppf ligand. When compared with the potential value reported for the behaviour of free dppf in solution [6,37], it is clear that the redox conversion of the dppf ligand in complex **2** requires higher overpotentials (about 0.44 V).

Contrasting the cyclic voltammograms of Fig. 2A- curve b and 2B, it can be seen that in compound **2** the peak currents relative to the Co(III)/Co(II) couple are much enhanced. This observation is consistent with the replacement of one carbonyl group by the phosphine ligand [38,39] upon coordination of dppf with $[Co(\eta^5-C_5H_5)(CO)_2]$.

3.3. Computational studies

DFT calculations [7] (Gaussian 03 [13]) were performed on the three complexes $[Co(\eta^5-C_5H_5)(CO)_2]$ (**1**), dppf, and $[Co(\eta^5-C_5H_5)(CO)]_2(\mu\text{-dppf})$ (**2**), and on the respective anions, monocations and dications, in order to understand the redox behaviour of the trinuclear complex **2**. All the geometries were optimised without symmetry constraints and the structural parameters (distances and angles) experimentally determined for **2** are well reproduced in calculations.
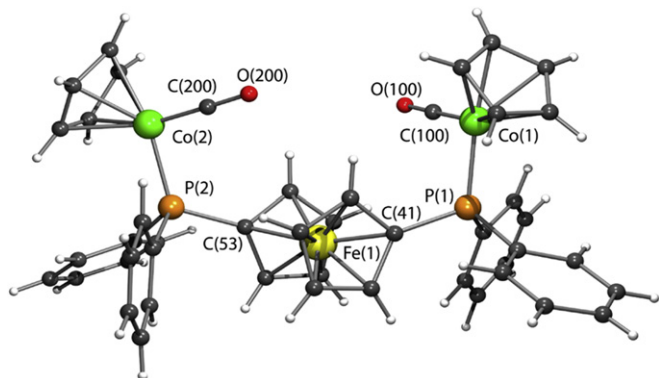
The comparison between the energy of the molecular orbitals (MO) of the three complexes is shown in Fig. 3 (labelled by the MO numbers for **1**, **1f**, and dppf, and by H, L, etc, for **2**). The most relevant feature of the diagram is the high energy of the HOMO compared with the energy of the HOMO of any of the two fragments. The highest occupied orbitals of **2** are mostly localised on the Co or in the Fe fragment.

The coordination of dppf to complex **1** involves only the donation from two phosphorus lone pairs, HOMO-2 (antisymmetric combination, MO 137) and HOMO-3 (symmetric combination, MO 136) in Scheme 2, to the acceptor orbitals of **1f** (MO 34), giving rise to low energy Co–P bonding levels and high energy Co–P antibonding ones (not shown). The occupied d-levels of dppf, respectively 139, 138,135, and 134, remain at almost the same energy as orbitals H-4, H-5, H-8, and H-9, of complex **2** (Fig. 3).

In terms of the cobalt fragment, the changes are much more dramatic. When dppf coordinates, one P atom of the phosphine replaces one carbonyl. It is more helpful thus to examine the frontier orbitals of the $Co(\eta^5-C_5H_5)(CO)$ fragment (**1f**) after the loss of CO.

Fig. 1. Molecular structure of $[Co(\eta^5-C_5H_5)(CO)]_2(\mu\text{-dppf})$, **2**, with two $Co(\eta^5-C_5H_5)(CO)$ moieties covalently linked by a dppf bridge.

Table 1
Selected bond lengths (Å) and angles (°) for $[Co(\eta^5-C_5H_5)(CO)]_2(\mu\text{-dppf})_2$.

|			
Co(1)–C(100)	1.683(14)	Co(2)–C(200)	1.678(7)
Co(1)–P(1)	2.140(3)	P(2)–Co(2)	2.141(4)
C(100)–O(100)	1.178(14)	C(200)–O(200)	1.175(3)
P(1)–C(41)	1.828(12)	P(2)–C(53)	1.835(12)
P(1)–C(21)	1.804(11)	P(2)–C(61)	1.815(12)
P(1)–C(31)	1.827(11)	P(2)–C(71)	1.832(14)
C(100)–Co(1)–P(1)	90.9(4)	C(200)–Co(2)–P(2)	94.5(2)
O(100)–C(100)–Co(1)	179.0(12)	O(200)–C(200)–Co(2)	178.2(4)
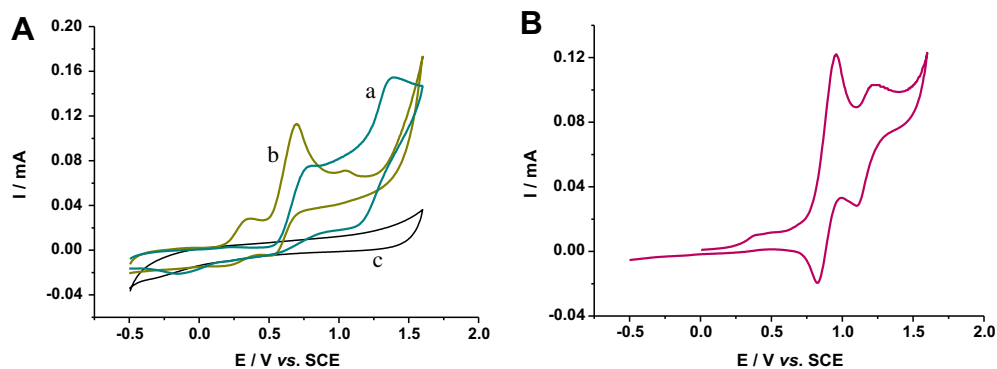
Fig. 2. Cyclic voltammograms (A) dppf (a) and **1**(b), and (B) **2** In CH_2Cl_2 containing 0.1 M $TBAPF_6$ as supporting electrolyte, Pt electrode, $\nu = 20$ mV s^{-1}; Pt electrode in 0.1 M $TBAPF_6$/ CH_2Cl_2 (A, curve c).
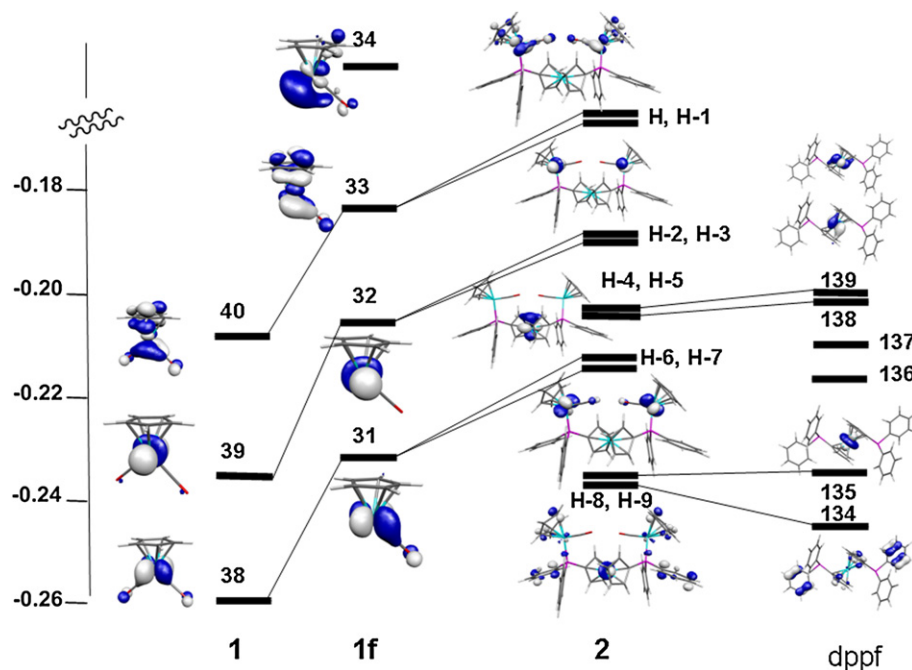
**Fig. 3.** Energy of the molecular orbitals of the three complexes **1**, dppf and **2**, and fragment **1f**.

The HOMO (40) of **1**, which is bonding between Co and the carbonyls (the bonding combination corresponding to back donation from the metal to the π-acceptor C≡O), loses part of its bonding character when CO is replaced by the phosphine and its energy rises significantly (33 of **1f**, Fig. 3). The same destabilisation is observed for both HOMO-1 (39 becomes 32 of **1f**) and HOMO-2 (38 becomes 31 of **1f**), as CO also contributed to them. The fragment **1f** has also a low energy empty orbital (LUMO), with the right symmetry to accept the

two electrons from the phosphine donor (MOs 136, 137 of dppf) and give rise to the Co–P σ bonding and σ* antibonding molecular orbitals (energies outside the range shown in Fig. 3). The HOMO (33) and HOMO-1 (32) of **1f** correspond to the HOMO, HOMO-1, HOMO-3 and HOMO-4 of **2**, still Co–CO bonding, but nonbonding on the side of the phosphine. Since there are two **1f** fragments in the trinuclear complex **2**, there are always pairs of molecular orbitals descending from the symmetric and asymmetric combinations. The asymmetric
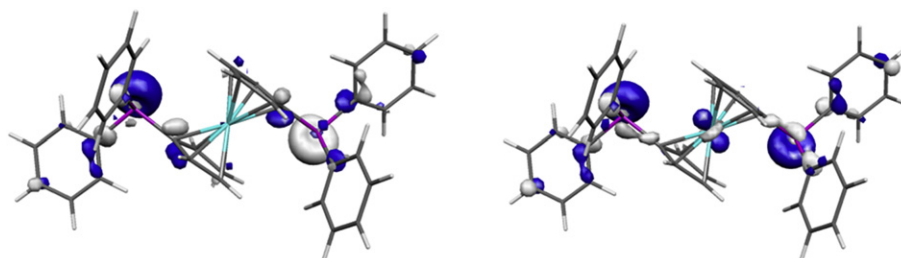
Scheme 2.
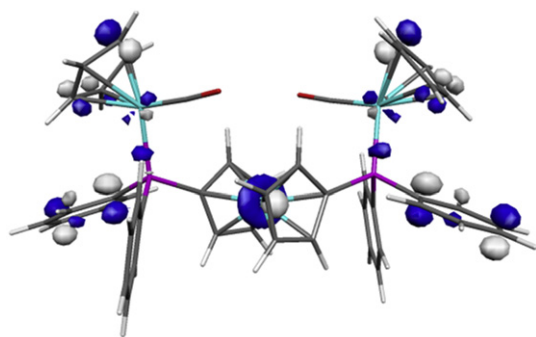
Scheme 3. HOMO-8 (197).

combinations are shown in Fig. 3. The four highest occupied MOs of complex **2** are localised on the cobalt fragments, without significant contribution of Fe. The same happens with HOMO-6 and HOMO-7. Orbitals deriving from those of dppf are the HOMO-8 and HOMO-9, but only in HOMO-8 (symmetric combination from 135, Scheme 3) is there a localisation on Fe, since 134 is localised on the Cp and phenyl groups. The HOMO-6 extending over the three metal centres, though with a very small contribution from the Co fragment, is shown in Scheme 3.

The order of the MOs of complex **2** does not change after the first oxidation, the highest occupied levels remaining localised on cobalt. These results suggest that the oxidation processes described above correspond to a double oxidation of Co in **1**, of Fe in dppf, and again in Co in the binuclear complex **2**. This results from the significant destabilisation of the molecular orbitals of **1** when a strong π-acceptor carbonyl is replaced by a strong σ-donor phosphine.

4. Conclusions

Reaction of $[Co(\eta^5\text{-}C_5H_5)(CO)_2]$ (**1**) with 1,1′-bis(diphenylphosphino)ferrocene (dppf) yields the new polynuclear compound $[Co(\eta^5\text{-}C_5H_5)(CO)]_2(\mu\text{-dppf})$, (**2**). The structure of complex **2** was determined by single crystal X-ray diffraction studies, and contains two $Co(\eta^5\text{-}C_5H_5)(CO)$ units covalently linked by a dppf bridge. The electrochemical study of **1**, dppf, and **2** shows that the mononuclear species are oxidised in dichloromethane solution (Co(I)/Co(II)/Co(III) and Fe(II)/Fe(III) in **1** and dppf, respectively). In the trinuclear species **2**, the first two oxidation processes observed correspond to Co(I)/Co(II) and Co(II)/Co(III) oxidations, whereas the oxidation of the dppf ligand takes place at higher potentials as compared with free dppf in solution. This behaviour arises from the substitution of a carbonyl by a phosphine in the coordination sphere of Co(I), leading to a much higher energy of the Co based molecular orbitals in **2**, as was confirmed by a DFT study.

Acknowledgements

Appendix A. Supplementary material

CCDC 614689 contains the supplementary crystallographic data for this paper. These data can be obtained free of charge from The Cambridge Crystallographic Data Centre via www.ccdc.cam.ac.uk/data_request/cif.

References

[1] a) K.P.C. Vollhardt, Angew. Chem. Int. Ed. Engl. 23 (1984) 539–556;
b) S. Saito, Y. Yamamoto, Chem. Rev. 100 (2000) 2901–2915;
c) F. Montilla, T. Avilés, T. Casimiro, A.A. Ricardo, M.N. da Ponte, J. Organomet. Chem. 632 (2001) 113–118.
[2] a) N. Agenet, V. Gandon, K.P.C. Vollhardt, M. Malacria, C. Aubert, J. Am. Chem. Soc. 129 (2007) 8860–8887;
b) L.F. Veiros, G. Dazinger, K. Kirchner, M.J. Calhorda, R. Schmid, Chem. Eur. J. 10 (2004) 5860–5870;
c) T. Avilés, S. Jansat, M. Martínez, F. Montilla, C. Rodríguez, Organometallics 30 (2011) 3919–3922;
d) C.-M. Weng, F.-E. Hong, Organometallics 30 (2011) 3740–3748.
[3] a) T. Avilés, M.L.H. Green, J. Chem. Soc. Dalton Trans. (1979) 1116–1120;
b) T. Avilés, P. Royo, J. Organomet. Chem. 221 (1981) 333–337;
c) T. Avilés, F. Barroso, P. Royo, J.H. Noordik, J. Organomet. Chem. 236 (1982) 101–108;
d) T. Avilés, F. Barroso, P. Royo, J. Organomet. Chem. 326 (1987) 423–429;
e) M.G. Teixeira, F. Paolucci, M. Marcaccio, T. Avilés, C. Paradisi, F. Maran, S. Roffia, Organometallics 17 (1998) 1297–1304;
f) T. Avilés, A. Dinis, M.J. Calhorda, P. Pinto, V. Félix, M.G.B. Drew, J. Organomet. Chem. 625 (2001) 186–194;
g) F. Montilla, V. Rosa, C. Prevett, T. Avilés, M. Nunes da Ponte, D. Masi, C. Mealli, J. Chem. Soc. Dalton Trans. (2003) 2170–2176;
h) F. Montilla, V. Rosa, T. Avilés, A. Galindo, Dalton Trans. (2004) 2588–2592;
i) M. Agostinho, V. Rosa, T. Avilés, R. Welter, P. Braunstein, Dalton Trans. (2009) 814–822.
[4] P. Pinto, M.J. Calhorda, V. Félix, T. Avilés, M.G.B. Drew, Monatsh. Chem. 131 (2000) 1253–1265.
[5] A. Togni, T. Hayashi, Ferrocenes, VCH, Weinheim, 1995.
[6] T. Avilés, A. Dinis, J.O. Gonçalves, V. Félix, M.J. Calhorda, A. Prazeres, M.G.B. Drew, H. Alves, R.T. Henriques, V. da Gama, P. Zanello, M. Fontani, J. Chem. Soc. Dalton Trans. (2002) 4595–4602.
[7] R.G. Parr, W. Young, Density Functional Theory of Atoms and Molecules, Oxford University Press, New York, 1989.
[8] J.J. Bishop, A. Davison, M.L. Katcher, D.W. Lichtenberg, R.E. Merrill, J.C. Smart, J. Organomet. Chem. 27 (1971) 241–249.
[9] M.D. Rauch, R.A. Genetti, J. Org. Chem. 35 (1970) 3888–3897.
[10] W. Kabsch, J. Appl. Cryst. 21 (1988) 916–924.
[11] G.M. Sheldrick, SHELX 97, University of Gottingen, 1997.
[12] A.L. Spek, J. Appl. Cryst. 36 (2003) 7.
[13] G. Trucks, H. Schlegel, G. Scuseria, M. Robb, J. Cheeseman, J. Montgomery Jr., T. Vreven, K. Kudin, J. Burant, J. Millam, et al., Gaussian 03, Revision C. 02, Gaussian. Inc., Wallingford, CT, 2004.
[14] A. Becke, J. Chem. Phys. 98 (1993) 5648–5652.
[15] C. Lee, W. Yang, R. Parr, Phys. Rev. B 37 (2) (1988) 785–789.
[16] S. Vosko, L. Wilk, M. Nusair, Can. J. Phys. 58 (8) (1980) 1200–1211.
[17] P. Stephens, F. Devlin, C. Chabalowski, M. Frisch, J. Phys. Chem. 98 (45) (1994) 11623–11627.
[18] L. Roy, H. Yang, R. Martin, J. Chem. Theor. Comput. 4 (7) (2008) 1029–1031.
[19] R. Ditcheld, W. Hehre, J. Pople, J. Chem. Phys. 54 (1971) 724–728.
[20] W. Hehre, R. Ditcheld, J. Pople, J. Chem. Phys. 56 (1972) 2257–2261.
[21] P. Hariharan, J. Pople, Theo. Chim. Acta 28 (3) (1973) 213–222.
[22] P. Hariharan, J. Pople, Mol. Phys. 27 (1974) 209–214.
[23] M. Gordon, Chem. Phys. Lett. 76 (1980) 163–168.
[24] E. Cances, B. Mennucci, J. Tomasi, J. Chem. Phys. 107 (8) (1997) 3032–3041.
[25] M. Cossi, V. Barone, B. Mennucci, J. Tomasi, Chem. Phys. Lett. 286 (3–4) (1998) 253–260.
[26] B. Mennucci, J. Tomasi, J. Chem. Phys. 106 (12) (1997) 5151–5158.
[27] J. Tomasi, B. Mennucci, R. Cammi, Chem. Rev. 105 (8) (2005) 2999–3094.
[28] M. Cossi, G. Scalmani, N. Rega, V. Barone, J. Chem. Phys. 117 (2002) 43–54.
[29] A. Bondi, J. Phys. Chem. 68 (3) (1964) 441–451.
[30] S. Portmann, H.P. Lüthi, Chimia 54 (2000) 766–770.
[31] J. Peng, C. L-K Liu, R. Chim. 5 (2002) 319–324.
[32] J.-F. Ma, Y. Yamamoto, J. Organomet. Chem. 574 (1999) 148–154.
[33] S. Onaka, T. Moriya, S. Takagi, A. Mizuno, H. Furuta, Bull. Chem. Soc. Jpn. 65 (1992) 1415–1427.
[34] F.H. Allen, Acta Crystallogr. B 58 (2002) 380–388.
[35] S. Onaka, M. Otsuka, A. Mizuno, S. Takagi, K. Sako, M. Otomo, Chem.Lett. (1994) 45–48.
[36] Z. Pang, X.-F. Huang, Z. Huang, F. R-Cai, R. Ruan, Synth. React. Inorg. Met.- Org. Chem. 30 (8) (2000) 1459–1476.
[37] A.E. Gerbase, E.J.S. Vichi, E. Stein, L. Amaral, A. Vasquez, M. Hörner, C. Maichle-Mössmer, Inorg. Chim. Acta 266 (1997) 19–27.
[38] F. X-Hou, Z. Pang, Y.-F. Xu, R.-F. Cai, Z.-E. Huang, Chin. J. Chem. 18 (2000) 733–739.
[39] Z. Pang, X.-F. Hou, Z.-E. Huang, R.-F. Cai, R. Ruan, Synth. React. Inorg. Met.- Org. Chem. 30 (8) (2000) 1459–1476.